Semiconductor physics

The influence of substrate temperature on the structure and optical properties of NiO thin films deposited using the magnetron sputtering in the layer-by-layer growth regime

A.I. Ievtushenko[1*], V.A. Karpyna[1], O.I. Bykov[1], M.V. Dranchuk[1], O.F. Kolomys[2], D.M. Maziar[2], V.V. Strelchuk[2], S.P. Starik[3], V.A. Baturin[4], O.Y. Karpenko[4], O.S. Lytvyn[5]

[1]*I. Frantsevich Institute for Problems of Materials Science, NAS of Ukraine, 03142 Kyiv, Ukraine*
[2]*V. Lashkaryov Institute of Semiconductor Physics, NAS of Ukraine, 03680 Kyiv, Ukraine*
[3]*V. Bakul Institute for Superhard Materials, NAS of Ukraine, 04074 Kyiv, Ukraine*
[4]*Institute of Applied Physics, NAS of Ukraine, 40000 Sumy, Ukraine*
[5]*Borys Grinchenko Kyiv University, 04053 Kyiv, Ukraine*
[*]*Corresponding author e-mail: a.ievtushenko@yahoo.com*

Abstract. Quality polycrystalline NiO films are very attractive materials for different applications. The effect of substrate temperature on the structure, morphology, and optical properties of NiO films deposited on glass substrates by using magnetron sputtering in the layer-by-layer growth regime has been considered. XRD pattern showed reflection from (111), (200), and (220) planes of cubic NiO. It has been demonstrated that the O/Ni stoichiometric ratio tends to 1.0 with increasing the substrate temperature. The optical transmittance of the deposited NiO films is within the range of 20 to 35%, while the optical band gap varies from 2.76 up to 2.98 eV. AFM analysis of the surface morphology revealed that the average grain size of the NiO films varied from 25 to 30 nm and surface roughness from 1.1 to 1.5 nm, respectively.

Keywords: NiO films, magnetron sputtering, XRD, substrate temperature, transmittance, atomic force microscopy.

https://doi.org/10.15407/spqeo26.04.398
PACS 77.55.-g, 78.20.-e, 81.15.Cd, 82.80.Pv

Manuscript received 25.08.23; revised version received 18.10.23; accepted for publication 22.11.23; published online 05.12.23.

1. Introduction

Nickel oxide (NiO) is a wide and direct band gap (E_g is in the range of 3.7 to 4.5 eV at room temperature) *p*-type semiconductor oxide crystallizing in a face-centered cubic lattice [1, 2]. The *p*-type conduction in NiO is related to the presence of the native point defects including nickel vacancies V_{Ni} and oxygen interstitial O_i [3, 4]. Due to stable structural and excellent chemical/ weather stability [5, 6], NiO films and nanostructures have been extensively studied in the recent few years because of their perspective for applications in smart windows [7], electrochromic coatings [8–10], perovskite solar cells as a *p*-type hole-transporting layer exhibiting high transparency and appropriate conductivity [11, 12], light-emitting diodes [13] and UV detectors [14, 15], energy-efficient coatings based on transparent heat mirrors [16], in gas sensors [17, 18], and in lithium-ion batteries as an anode material [19], *etc*. Therefore, the development of technology for NiO films growth with high structure and optical quality having required conductivity is needed.

There are many technologies for NiO films deposition, namely: plasma-enhanced chemical vapour deposition [20], magnetron sputtering [21], pulsed laser deposition [22], electron beam evaporation [23], electrochemical deposition [24] and spray pyrolysis [25, 26]. Among these mentioned growth methods, reactive magnetron sputtering (MS) is considered to be the most widely used due to good film adhesion, high deposition rates, film uniformity over large areas of the substrates and easy control over the composition of the deposited films [27].

It is clear that the improvement of NiO film properties can be reached by the optimization of their deposition parameters as well as applications of new technological approaches for films condensation.

© V. Lashkaryov Institute of Semiconductor Physics of the NAS of Ukraine, 2023
© Publisher PH "Akademperiodyka" of the NAS of Ukraine, 2023

Early, we proposed the layer-by-layer growth method for magnetron sputtering undoped and doped ZnO films [26, 28, 29]. This approach allowed us to improve film crystal quality as compared to that of films deposited in traditional single-stage magnetron sputtering. In this paper, we consider the effect of substrate temperature on the structure and optical properties of NiO films deposited on glass substrates by using the layer-by-layer growth method at magnetron sputtering.

2. Experimental

2.1. Sample preparation

NiO thin films were grown on glass and Si substrates employing the layer-by-layer growth regime at reactive magnetron sputtering of nickel metallic target with purity 99.99% in the oxygen-argon atmosphere. Vacuum equipment VS350 operating with a turbomolecular pump and separate gas inlets were used. The layer-by-layer NiO film growth consists of three stages of this growth with technological stops between them (when the magnetron is turned off). The total time of film deposition was 6 min (*i.e.*, three stages lasting two minutes of growth). The magnetron power, argon and oxygen pressures were fixed as 250 W, 1.0 Pa, and 0.7 Pa, respectively. We changed the substrate temperature as follows: 150, 250 and 350 °C.

2.1. Characterization

The crystal structure of deposited NiO films was investigated with X-ray diffraction (XRD) by using the DRON-4 diffractometer utilizing Cu-K_α radiation ($\lambda = 0.1542$ nm). The elemental analysis of NiO films was realized with ZEISS EVO 50 XVP SEM by using energy dispersive X-ray spectroscopy (EDX) furnished by INCA 450 (OXFORD Instruments). The surface morphology of the deposited films was analyzed using the atomic force microscope (AFM) NanoScope IIIa Dimension 3000 (Digital Instruments/Bruker, USA) operated in tapping mode. The AFM measurements were performed using silicon tips with a nominal tip apex radius of 10 nm. Transmittance of NiO films deposited onto glass substrates was investigated by Shimadzu UV-Visible Spectrophotometer UV-2600i (Japan). The FTIR reflectance measurement has been performed with the vacuum Fourier transform spectrometer Bruker Vertex 70V at room temperature. For each spectrum, the number of scans was 64, the spectral resolution – 1 cm^{-1}. For reflectance measurements, as a reference a gold mirror was used. The resistivity of NiO films was studied using the Van der Pauw method in the dark with Keithley-236 Source Measure Unit.

3. Results and discussion

X-ray diffraction patterns (Fig. 1) reveal the XRD reflection from (111), (200) and (220) crystallographic planes of cubic NiO films (in accord with JCPDS card no: 78-0643), deposited in the layer-by-layer growth regime of magnetron sputtering onto glass substrates

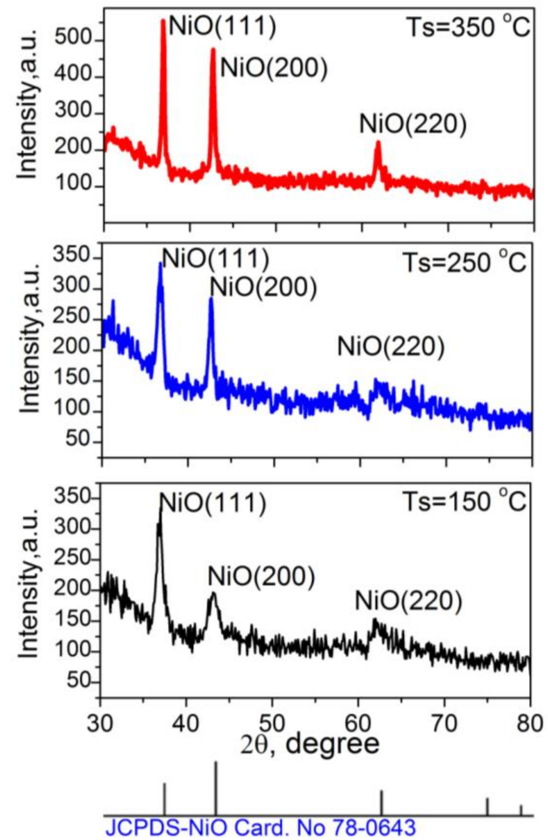

Fig. 1. X-ray diffraction patterns of NiO films grown on glass substrates at various substrate temperatures.

at various substrate temperatures. Therefore, NiO films deposited by magnetron sputtering are polycrystalline single-phase materials with NaCl-type structure.

For a more detailed analysis of the structure of NiO films, the Gauss approximation of the most intensive XRD (111) peak was performed, and its peak position and the full width at half maximum (FWHM) values were found (Table). The lattice parameter a for the cubic structure of NiO can be calculated from XRD data by using the equation [28]:

$$\frac{1}{d_{hkl}^2} = \frac{h^2 + k^2 + l^2}{a^2} , \quad (1)$$

where d_{hkl} is the interplanar distance between adjacent planes in the set (hkl), a is the lattice parameter, and h, k and l are the indices of the planes. NiO has a face-centered cubic (Fm–$3m$) structure [31]. Lattice constants a calculated from (111) reflexes are larger than the reference value for NiO single crystal with the lattice parameter $a_0 = 0.4177$ nm. The stress developed in the films was calculated using the X-ray diffraction data in accord with the following relation [32]:

$$\sigma = -\frac{E}{2\nu}\left(\frac{a - a_0}{a_0}\right), \quad (2)$$

where E is the Young modulus of the NiO (200 GPa),

Table. The results of XRD analysis of NiO films.

Substrate temperature, °C	Position of (111) peak, degree	FWHM of (111) peak, degree	Interplanar spacing d, nm	Lattice parameter a, nm	Stress, GPa	Size of crystallites, nm
150	36.91	0.77	0.2435	0.4218	–3.15	11
250	36.74	0.70	0.2446	0.4237	–4.61	12
350	36.90	0.32	0.2436	0.4219	–3.24	26

a and a_0 is the lattice parameter of the film and bulk material, respectively, and ν is the Poisson ratio (0.31) [33]. The grain size (D) was evaluated using the Scherrer formula [34]:

$$D = \frac{0.9\lambda}{\beta\cos\theta}, \quad (3)$$

where D is the size of crystallites, λ equals X-ray radiation wavelength, β is FWHM of diffraction peak, and θ is the Bragg angle.

The results of calculating the size of crystallites in the NiO films as a function of the substrate temperature are shown in Table. It can be seen that with an increase in the substrate temperature, the size of crystallites increases from 11 to 26 nm, which is obviously caused by the crystalline quality of NiO films being enhanced and the reduction of the concentration of native defects and dislocations. Hence, with increasing the substrate temperature, the crystallinity of the films is improved and the size of crystallites becomes larger. The stress of NiO films grown on glass substrates was in the range of –3.15 to –4.61 GPa. These large values of stress obviously were related to the amorphous nature of the glass substrate as well as to different thermal expansion coefficients between film and glass substrate, which leads to formation of native defects and dislocations in NiO films [35]. The XRD data and calculated values of lattice parameters, film stresses and size of crystallites are summarized in Table.

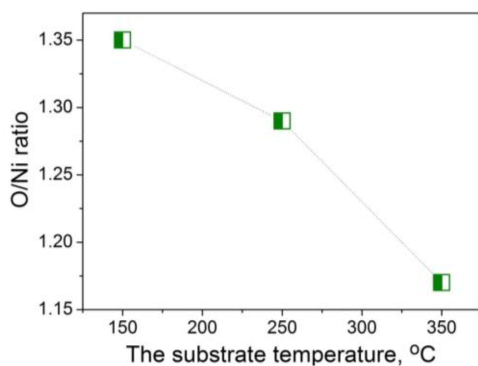

Fig. 2. Variations of the O/Ni ratio in NiO films as a function of substrate temperature.

Fig. 2 displays variations of the O/Ni ratio in NiO films as a function of substrate temperature. The EDX measurements confirm that NiO film samples contain no other elements except nickel and oxygen [36]. No additional peaks of impurities are revealed. It can be seen that the O/Ni ratio tends to 1.0 with increasing the substrate temperature, which is consistent with the results of XRD studies, when we also observed an enhancement of size of crystallites in NiO films with increasing the temperature of glass substrate.

Fig. 3a shows the transmission spectra of NiO films as a function of substrate temperature. The absorption spectra in Tauc coordinates of the deposited NiO films

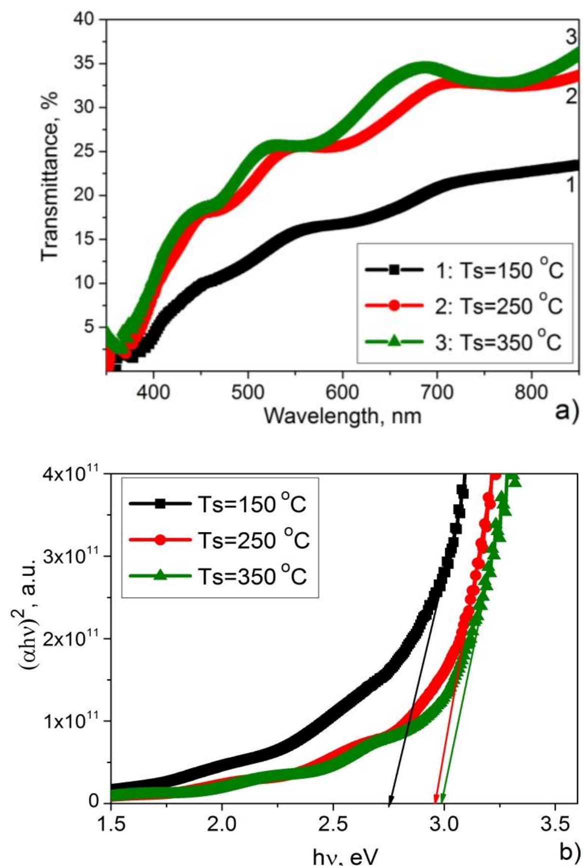

Fig. 3. Optical transmittance (a) and absorption spectra in Tauc coordinates (b) of the NiO films deposited on glass substrates as a function of substrate temperature. (Color online)

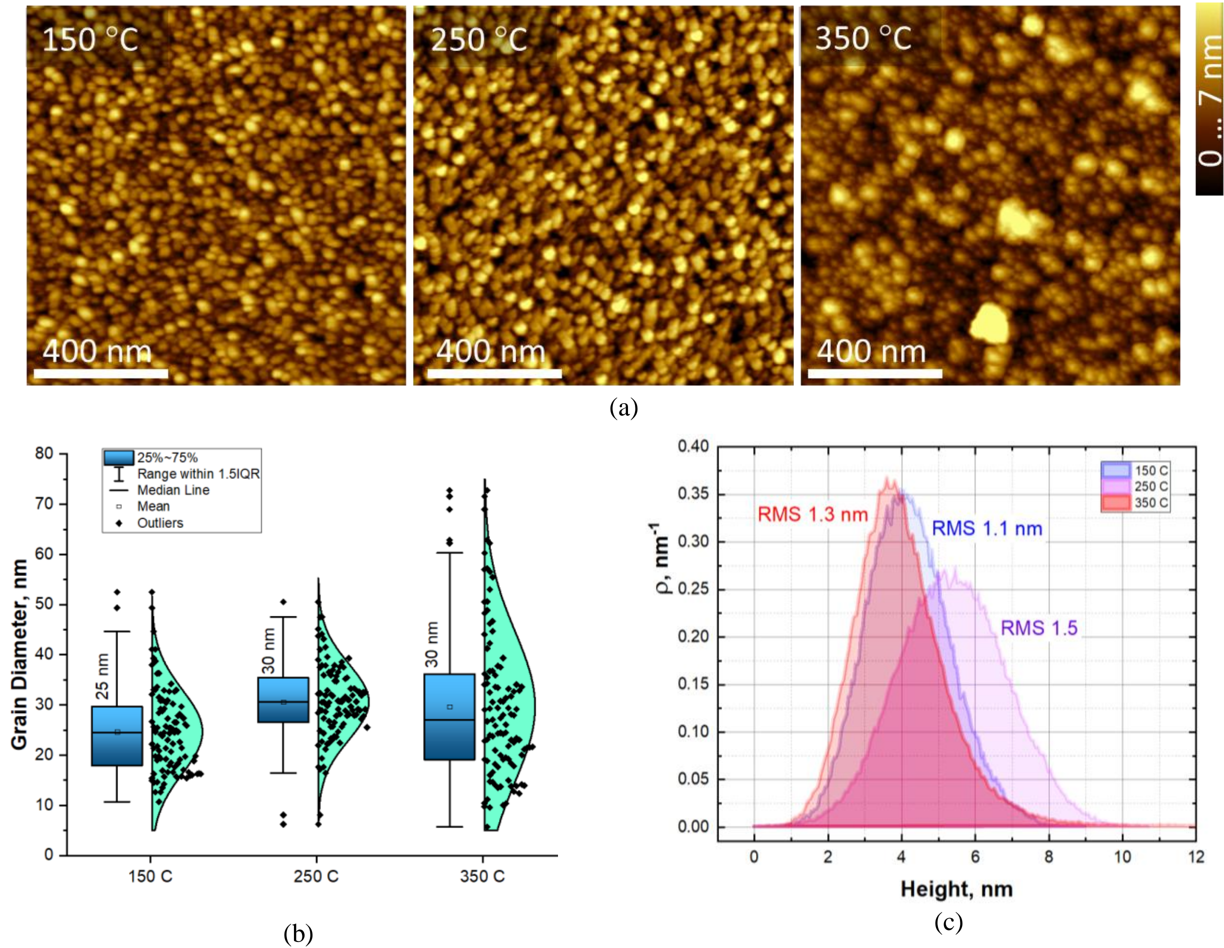

Fig. 4. AFM height images (a), boxplots for grain diameters and corresponding distributions (b), height histograms (over 1.2×1.2 µm) (c) of NiO films, all as a functions of substrate temperature. (Color online)

are shown in Fig. 3b. For the direct transition, the optical band gap (E_g) can be obtained by using the Tauc relationship:

$$\alpha = A\frac{(h\nu - E_g)^{1/2}}{h\nu}\,, \qquad (4)$$

where α is the absorption coefficient, *A* is the constant, and $h\nu$ is the photon energy. The band gaps obtained by extrapolating the straight-line portion of $(\alpha h\nu)^2$ *vs* $h\nu$ plots to the *x*-axis are depicted with inserts in Fig. 3b.

As can be seen in Fig. 3, the substrate temperature affects the average transmittance which increases from 20 to 35% in the visible part of the spectrum 400…800 nm with the substrate temperature increase from 150 up to 350 °C. It is important that the transmittance of NiO films correlates with changing the values of crystallite sizes, namely, the highest transparency and, accordingly, a smaller number of scattering centers (defects) are observed in oxide films grown at the highest substrate temperatures. With an increase in the substrate temperature from 150 to 350 °C, the optical band gap increases from 2.76 to 2.98 eV, respectively (Fig. 3b). In Ref. [31], it was shown that the optical band gap of NiO films depends on the method of deposition and its parameters. Hence, the observed increase of optical band gap with substrate temperature is due to an improvement in the NiO film structure (decreasing native defects – nickel vacancies, which correlated with elemental composition for the oxide films as well as dislocations density).

Fig. 4 presents the AFM images of the surface morphology, along with an analysis of the distribution of grain diameters and surface heights of the deposited NiO films, as a function of substrate temperature. In Fig. 4b, for each value of substrate temperature, a boxplot is shown. This boxplot includes data with an interquartile range (IQR, 25%...75%), whiskers drawn within the 1.5 IQR value, the mean/median grain diameter, data in bins (represented as black dots), and corresponding normal distributions. Fig. 4c displays the heights histograms and the root-mean-square roughness (RMS) values for each film.

The surfaces are composed of densely packed nanosized grains. The surface of the film deposited at the substrate temperature 150 °C is uniform, with grain diameters ranging within 10…45 nm (range with outliers removed), as depicted in Fig. 4b. The mean grain

diameter is 25 nm, and the surface height varies from 1 to 8 nm across a 1.2×1.2 μm area, peaking at 4 nm, with the RMS value close to 1.1 nm (Fig. 4c). The grain sizes on the surface of the film deposited at the substrate temperature 250 °C have slightly increased (the range has shifted to 15…47 nm, with a mean value close to 30 nm). Here is the smallest interquartile range, while RMS of 1.5 nm is the highest. The surface of the film deposited at the substrate temperature 350 °C is most distinctive: although the mean grain diameter remains 30 nm, the surface is heterogeneous, with grain sizes ranging from 5 up to 60 nm. The interquartile range of the grain diameter distribution is maximal, the peak of the surface height distribution is the smallest at 3.5 nm (RMS of 1.3 nm), but the asymmetric tail is presented from the side of higher values. An analysis of the type of grain distribution by their diameter (Fig. 4b) revealed that the distribution in the film obtained at the substrate temperature 250 °C is closest to the normal one. In the films corresponding to the substrate temperatures 150 and 350 °C, the distribution is close to the log-normal one with deviation of surface grain diameters towards larger sizes from the mean value.

Fig. 5 presents the infrared absorption spectra for all the prepared NiO films in the range 100 to 1000 cm^{-1}. The IR spectra of NiO films showed the presence of two asymmetrical broad absorption maxima – one at ~386 cm^{-1}, which corresponds to transverse optical phonon (TO), and the other at 570 cm^{-1} may be assigned to longitudinal optical phonon (LO) of NiO that related to the oscillations of the Ni^{2+} ions sublattice at the angle 180° opposite to the O^{2-} ions sublattice [37]. The small absorption maxima of about 540 cm^{-1} were identified as a surface mode (SM) [38]. With increasing the growth temperature, the IR band of Ni–O stretching vibration broadened and shifted to the short-wave range due to the quantum size effect [39]. Strong absorption is observed for the NiO films deposited at higher substrate temperatures, which implies better crystalline structure (higher values for the size of crystallites in NiO films) as compared to the ones deposited at low substrate temperatures.

The dependence of resistivity for the NiO films on the O/Ni ratio is shown in Fig. 6. With increasing the substrate temperature as well as with decreasing the O/Ni ratio, the electrical resistivity of NiO films increases from 0.43 up to 3.7 Ohm·cm. The type of conductivity of grown NiO films was examined by the heat probe method. It was shown that all the NiO film deposited in the substrate temperature range 150...350 °C demonstrated *p*-type conductivity. As shown in [40], the resistivity of NiO films depends on the concentration of Ni vacancies (V_{Ni}), which determines the hole conductivity of NiO [41]. Also, Ni^{3+} ion corresponds to the nickel vacancy and the acceptor in the NiO lattice [42]. The enhancement of the resistivities of NiO films deposited with the rise in the substrate temperatures could be explained by reducing the concentration of Ni vacancies (concentrations of hole carriers) due to the improvement of the O/Ni ratio (Fig. 6).

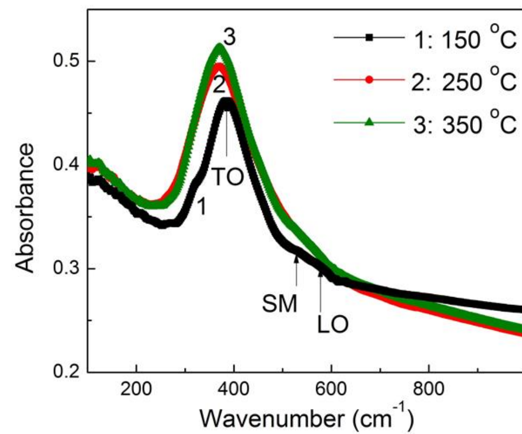

Fig. 5. Infrared absorption spectra of deposited NiO films as a function of substrate temperature. (Color online)

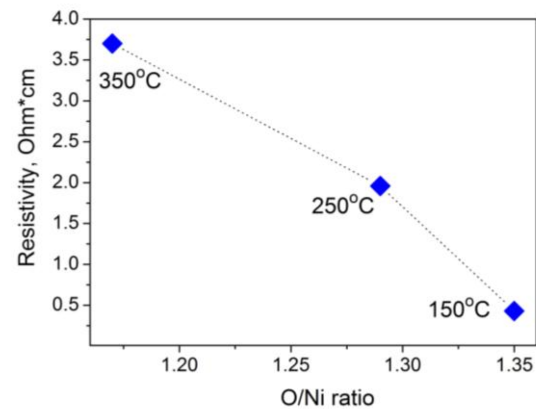

Fig. 6. Resistivity of NiO films *versus* O/Ni ratio. The value of the temperature of the substrate is included into the figure.

The resistivity values (0.43 to 3.7 Ohm·cm) of NiO films are comparable to those reported by Lu *et al*. [43] and Lei Ai *et al*. [44].

The SEM image of NiO/glass profile shown in Fig. 7 demonstrates the uniformity of three-layered NiO film grown on the glass substrate at 350 °C. The thickness of NiO films was close to 460 nm. As we can see, the NiO film surface is flat, and the columnar growth of NiO films was observed. It should be noted that the application of the layer-by-layer regime at NiO film deposition does not lead to appearance of cracks and pores as can be seen in the cross-section view (Fig. 7).

Hence, for the first time, we applied the layer-by-layer regime in rf magnetron sputtering to deposit the NiO films onto amorphous glass substrates. All the grown NiO films deposited at the varied substrate temperature between 150 and 350 °C were polycrystalline single-phase materials with NaCl-type structure with a preferred orientation of NiO crystallites (111). With increasing the substrate temperature, the intensity of the XRD peak of NiO (200) gradually increases, while the intensity of the XRD peak (111) practically does not change.

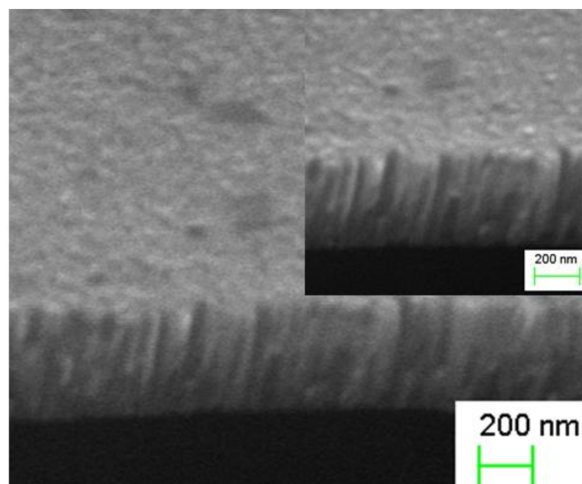

Fig. 7. SEM cross-section image of NiO film/glass substrate with the inset of an enlarged image.

Our obtained results indicate that the preferred orientation of crystallites in NiO films slightly changes with increasing substrate temperatures (the texture coefficient (111) becomes less pronounced). Lei Ai *et al.* [44] observed a transition from amorphous to polycrystalline structures with different preferred orientations of NiO (100) and (111) for the NiO films grown on crystalline Si substrates at increasing the substrate temperatures from the room one up to 400 °C. As compared with our results, Lin-Yan Xie *et al.* [45] obtained a completely different behaviour of the diffraction peaks of the thin NiO films with increasing the substrate temperature, namely: the diffraction peak of NiO (111) becomes intense, however, the diffraction peak of NiO (100) weakens with increasing the substrate temperature. Thus, with increasing the substrate temperature, orientation of crystallites in NiO films along the (111) becomes more pronounced.

In general, crystallography of a NaCl-type structure of NiO films is influenced by localization of oxygen ions, when the active species are nickel and oxygen, which are formed during the sputtering process [46]. When the substrate temperature increases, the surface reactivity of the reactant species is enhanced, thus promoting nucleation and growth of NiO grains. Also, the crystallographic texture of the NiO film is usually affected by the arrangement of O^{2-} ions (depending on oxygen pressure in the deposition chamber) [46]. At a lower substrate temperature, the sputtering process may result in formation of fewer reactive oxygen species due to plasma decomposition of O_2 molecules than at a higher temperature. In an oxygen-deficient environment, the (200) plane is the most densely packed plane among the planes composed of both Ni^{2+} and O^{2-} for the NiO crystal structure, indicating that the (200) orientation reduces the surface free energy of growing nickel oxide films [44, 46]. At higher deposition temperatures, there is a sufficient amount of reactive oxygen species, the (111) plane being the most densely packed plane of oxygen ions, resulting in a (111)-textured structure [44, 46]. It is important that Lei Ai *et al.* [44] deposited NiO films at the relative oxygen partial pressure $O_2/(Ar + O_2)$ of 60% and magnetron power of 250 W. In our investigation, the relative oxygen partial pressure $O_2/(Ar + O_2)$ was about 41%, and magnetron power of 250 W. Unfortunately, in the work of Lei Ai *et al.* [44] the O/Ni ratio of NiO films was not determined. Therefore, we can suppose that the observed increasing intensities of crystallites along (200) in NiO with increasing the temperature were caused by the oxygen-deficient environment in a deposition chamber.

In summary, application of the layer-by-layer regime in magnetron sputtering allows us to grow uniform polycrystalline single-phase NiO films on amorphous glass substrate even at low substrate temperatures. We proposed that the positive role of interruptions consists in the possibility of Ni and O adatoms to take up their true positions in forming crystal NiO structure. It leads to decreasing the number of NiO surface defects and favors homoepitaxial growth of NiO layer on NiO [27, 28]. In other words, the proposed layer-by-layer regime allows for the improvement of the structure of films by reducing lattice misfit between growth films and substrate by applying the process “interruption – homoepitaxy”.

4. Conclusions

This study enables to ascertain the impact of substrate temperature on the structure, morphology, and optical properties of NiO films deposited using the magnetron sputtering in the layer-by-layer growth regime. The optical transmittance of the deposited NiO films with the thickness close to 460 nm lies within the range from 20 up to 35%, and the optical band gap varies from 2.76 to 2.98 eV. Our AFM analysis has revealed that the mean grain size and surface roughness of the NiO films vary from 25 to 30 nm and from 1.1 to 1.5 nm, respectively. It has been shown that NiO films deposited using the layer-by-layer magnetron sputtering exhibit appropriate structure and optical properties for various applications.

Acknowledgements

The authors are sincerely grateful to all defenders of Ukraine and emergency workers who made it possible to perform these studies and publish our scientific results.

References

1. Ukoba O., Eloka-Eboka A.C., Inambao F.L. Review of nanostructured NiO thin film deposition by using the spray pyrolysis technique. *Renew. Sust. Energ. Rev.* 2018. **82**. P. 2900–2915. https://doi.org/10.1016/j.rser.2017.10.041.
2. Zhao J., Tian Y., Liu A., Song L., Zhao Z. The NiO electrode materials in electrochemical capacitor: A review. *Mater. Sci. Semicond. Process.* 2019. **96**. P. 78–90. https://doi.org/10.1016/j.mssp.2019.02.024.

3. Hwang J.D., Ho T.H. Effects of oxygen content on the structural, optical, and electrical properties of NiO thin films fabricated by radio-frequency magnetron sputtering. *Mater. Sci. Semicond. Process.* 2017. **71**. P. 396–400. https://doi.org/10.1016/j.mssp.2017.09.002.
4. Gao X., Meng X. Effect of reactive pressure on direct current-sputtered NiO films with improved *p*-type conduction ability. *Phys. B: Condens. Matter.* 2023. **650**. P. 414540. https://doi.org/10.1016/j.physb.2022.414540.
5. Chen H., Ma H., Xia H. *et al*. Optimization parameters of NiO films by DC magnetron sputtering and improvement of electrochromic properties by a mixed electrolyte. *Opt. Mater.* 2021. **122**. P. 111639. https://doi.org/10.1016/j.optmat.2021.111639.
6. Ievtushenko A., Karpyna V., Khyzhun O. *et al*. The effect of magnetron power and oxygen pressure on the properties of NiO films deposited by magnetron sputtering in layer-by-layer growth regime. *Vacuum*. 2023. **215**. P. 112375. https://doi.org/10.1016/j.vacuum.2023.112375.
7. Phan G.T., Pham D.V., Patil R.A. *et al*. Fast-switching electrochromic smart windows based on NiO-nanorods counter electrode. *Sol. Energy Mater. Sol. Cells*. 2021. **231**. P. 111306. https://doi.org/10.1016/j.solmat.2021.111306.
8. Huang H., Lu S.X., Zhang W.K. *et al*. Photoelectrochromic properties of NiO film deposited on an N-doped TiO_2 photocatalytical layer. *J. Phys. Chem. Solids*. 2009. **70**. P. 745–749. https://doi.org/10.1016/j.jpcs.2009.03.002.
9. Xu W., Mao X., Zhou N. *et al*. Effects of atomic oxygen on the growth of NiO films by reactive magnetron sputtering deposition. *Vacuum*. 2022. **196**. P. 110785. https://doi.org/10.1016/j.vacuum.2021.110785.
10. Sawaby A., Selim M.S., Marzouk S.Y. *et al.* Structure, optical and electrochromic properties of NiO thin films. *Phys. B: Condens. Matter.* 2010. **405**, No 16. P. 3412–3420. https://doi.org/10.1016/j.physb.2010.05.015.
11. Xu L., Chen X., Jin J. *et al.* Inverted perovskite solar cells employing doped NiO hole transport layers: A review. *Nano Energy*. 2019. **63**. P. 103860. https://doi.org/10.1016/j.nanoen.2019.103860.
12. Wang K.-C., Shen P.-S., Li M.-H. *et al.* Low-temperature sputtered nickel oxide compact thin film as effective electron blocking layer for mesoscopic NiO/$CH_3NH_3PbI_3$ perovskite heterojunction solar cells. *ACS Appl. Mater. Int.* 2014. **6**. P. 11851. https://doi.org/10.1021/am503610u.
13. Jung B.O., Kwon Y.H., Seo D.J. *et al.* Ultraviolet light emitting diode based on *p*-NiO/*n*-ZnO nanowire heterojunction. *J. Cryst. Growth.* 2013. **370**. P. 314–318. https://doi.org/10.1016/j.jcrysgro.2012.10.037.
14. Echresh A., Chey C.O., Shoushtari M.Z. *et al*. UV photodetector based on *p*-NiO thin film/*n*-ZnO nanorods heterojunction prepared by a simple process. *J. Alloy. Compd.* 2015. **632**. P. 165–171. https://doi.org/ 10.1016/j.jallcom.2015.01.155.
15. Xu J., Cao R., Shi S. *et al.* Self-powered ultraviolet photodetectors based on match like quasi one-dimensional *n*-TiO_2/*p*-NiO core-shell heterojunction arrays with NiO layer sputtered at different power. *J. Alloys Compd.* 2022. **928**. P. 167126. https://doi.org/10.1016/j.jallcom.2022.167126.
16. Al-Kuhaili M.F., Ahmad S.H.A., Durrani S.M.A. *et al*. Application of nickel oxide thin films in NiO/Ag multilayer energy-efficient coatings. *Mater. Sci. Semicond. Process.* 2015. **39**. P. 84–89. https://doi.org/10.1016/j.mssp.2015.04.049.
17. Mokoena T.P., Swart H.C., Motaung D.E. A review on recent progress of *p*-type nickel oxide based gas sensors: Future perspectives. *J. Alloys Compd.* 2019. **805**. P. 267–294. https://doi.org/10.1016/j.jallcom.2019.06.329.
18. Mokoena T.P., Hillie K.T., Swart H.C. *et al.* Fabrication of a propanol gas sensor using *p*-type nickel oxide nanostructures: the effect of ramping rate towards luminescence and gas sensing characteristics. *Mater. Chem. Phys.* 2020. **253**. P. 123316. https://doi.org/10.1016/j.matchemphys.2020.123316
19. Ma L., Pei X.-Y., Mo D.-C. *et al*. Fabrication of NiO-ZnO/RGO composite as an anode material for lithium ion batteries. *Ceram. Int.* 2018. **44**. P. 22664. https://doi.org/10.1016/j.ceramint.2018.09.044.
20. Wang H., Wua G., Cai X.P. *et al.* Effect of growth temperature on structure and optical characters of NiO films fabricated by PA-MOCVD. *Vacuum*. 2012. **86**. P. 2044. https://doi.org/10.1016/j.vacuum.2012.05.006.
21. Chen S.C., Wen C.K., Kuo T.Y., Peng W.C., Lin H.C. Characterization and properties of NiO films produced by rf magnetron sputtering with oxygen ion source assistance. *Thin Solid Films*. 2014. **572**. P. 51–55. https://doi.org/10.1016/j.tsf.2014.07.062.
22. Fasaki I., Koutoulaki A., Kompitsas M., Charitidis C. Structural, electrical and mechanical properties of NiO thin films grown by pulsed laser deposition. *Appl. Surf. Sci.* 2010. **257**. P. 429–433. https://doi.org/10.1016/j.apsusc.2010.07.006.
23. Pereira S., Gonçalves A., Correia N. *et al.* Electrochromic behavior of NiO thin films deposited by e-beam evaporation at room temperature. *Sol. Energ. Mat. Sol. C.* 2014. **120**. P. 109–115. https://doi.org/10.1016/j.solmat.2013.08.024.
24. Sonavane A.C., Inamdar A.I., Shinde P.S. *et al.* Efficient electrochromic nickel oxide thin films by electrodeposition. *J. Alloys Compd.* 2010. **489**. P. 667. https://doi.org/10.1016/j.jallcom.2009.09.146.
25. Kate R.S., Bulakhe S.C., Deokate R.J. Effect of substrate temperature on properties of nickel oxide (NiO) thin films by spray pyrolysis. *J. Electron. Mater.* 2019. **48**. P. 3220–3228. https://doi.org/10.1007/s11664-019-07074-0.

26. Reguig B.A., Khelil A., Cattin L. *et al*. Properties of NiO thin films deposited by intermittent spray pyrolysis process. *Appl. Surf. Sci*. 2007. **253**. P. 4330–4334. https://doi.org/10.1016/j.apsusc.2006.09.046.
27. Ievtushenko A.I., Karpyna V.A., Lazorenko V.I. *et al.* High quality ZnO films deposited by radio-frequency magnetron sputtering using layer by layer growth method. *Thin Solid Films.* 2010. **518**. P. 4529–4532. https://doi.org/10.1016/j.tsf.2009.12.023.
28. Ievtushenko A.I., Lashkarev G.V., Lazorenko V.I. *et al.* Effect of nitrogen doping on photoresponsivity of ZnO films. *phys. status solidi (a)*. 2010. **207**. P. 1746–1750. https://doi.org/10.1002/pssa.200983750.
29. Karpyna V., Ievtushenko A., Kolomys O. *et al.* Raman and photoluminescence study of Al, N-Co doped ZnO films deposited at oxygen-rich conditions by magnetron sputtering. *phys. status solidi* (*b*). 2020. **257**. P. 1900788. https://doi.org/10.1002/pssb.201900788.
30. Salunkhe P., Ali M.A.V., Kekuda D. Structural, spectroscopic and electrical properties of dc magnetron sputtered NiO thin films and an insight into different defect states. *Appl. Phys. A.* 2021. **127**. P. 390. https://doi.org/10.1007/s00339-021-04501-0.
31. Fiévet F., Germi P., De Bergevin F., Figlarz M. Lattice parameter, microstrains and non-stoichiometry in NiO. Comparison between mosaic microcrystals and quasi-perfect single micro-crystals. *J. Appl. Cryst*. 1979. **12**. P. 387–394. https://doi.org/10.1107/S0021889879012747.
32. Ohring M. *The Material Science of Thin Solid Films*. Academic Press, New York, 1992.
33. Reddy A.M., Reddy A.S., Lee K.-S., Reddy P.S. Growth and characterization of NiO thin films prepared by dc reactive magnetron sputtering. *Solid State Sci*. 2011.**13**. P. 314–320. https://doi.org/10.1016/j.solidstatesciences.2010.11.019.
34. Cullity B.D. *Elements of X-ray Diffraction* (3rd Ed.). Addison-Wesley, Reading, MA, 1967.
35. Zhu B.L., Sun X.H., Guo S.S. *et al*. Effect of thickness on the structure and properties of ZnO thin films prepared by pulsed laser deposition. *Jpn. J. Appl. Phys.* 2006. **45**. P. 7860. https://doi.org/10.1016/10.1143/JJAP.45.7860.
36. Anand G.T., Nithiyavathi R., Ramesh R. *et al*. Structural and optical properties of nickel oxide nanoparticles: Investigation of antimicrobial applications. *Surf. Interfaces*. 2020. **18**. P.100460. https://doi.org/10.1016/j.surfin.2020.100460.
37. Wang Y., Saal J.E., Wang J.-J. *et al*. Broken symmetry, strong correlation, and splitting between longitudinal and transverse optical phonons of MnO and NiO from first principles. *Phys. Rev. B*. 2010. **82**. P. 081104(R). https://doi.org/10.1103/PhysRevB.82.081104.
38. Biju V., Khadar M. A. Fourier transform infrared spectroscopy study of nanostructured nickel oxide. *Spectrochim. Acta A Mol. Biomol. Spectrosc.* 2003. **59**. P. 121–134. https://doi.org/10.1016/S1386-1425(02)00120-8.
39. Duan W.J., Lu S.H., Wu Z. L., Wang Y.S. Size effects on properties of NiO nanoparticles grown in alkalisalts. *J. Phys. Chem. C.* 2012. **116**. P. 26043–26051. https://doi.org/10.1021/jp308073c.
40. Wittenhauer M.A., Van Zandt L.L. Surface conduction versus bulk conduction in pure stoichiometric NiO crystals. *Philos. Mag. B.* 1982. **46**. P. 659–667. https://doi.org/10.1080/01418638208223551.
41. Choi J.-M., Im S. Ultraviolet enhanced Si-photodetector using *p*-NiO films. *Appl. Surf. Sci.* 2005. **244**. P. 435–438. https://doi.org/10.1016/j.apsusc.2004.09.152.
42. Chang H.L., Lu T.C., Kuo H.C., Wang S.C. Effect of oxygen on characteristics of nickel oxide/indium tin oxide heterojunction diodes. *J. Appl. Phys Lett.* 2006. **100**. P. 124503. https://doi.org/10.1063/1.2404466.
43. Lu Y.M., Hwang W.S., Yang J.S., Chuang H.C. Properties of nickel oxide thin films deposited by RF reactive magnetron sputtering. *Thin Solid Films*. 2002. **420–421**. P. 54–61. https://doi.org/10.1016/S0040-6090(02)00654-5.
44. Ai L., Fang G., Yuan L. *et al.* Influence of substrate temperature on electrical and optical properties of p-type semitransparent conductive nickel oxide thin films deposited by radio frequency sputtering. *Appl. Surf. Sci*. 2008. **254**. P. 2401–2405. https://doi.org/10.1016/j.apsusc.2007.09.051.
45. Xie L.-Y., Xiao D.-Qi., Pei J.-X. *et al.* Growth, physical and electrical characterization of nickel oxide thin films prepared by plasma-enhanced atomic layer deposition using nickelocene and oxygen precursors. *Mater. Res. Express.* 2020. **7**. P. 046401. https://doi.org/10.1016/10.1088/2053-1591/ab82c9.
46. Ryu H.W., Choi G.P., Hong G.J., Park J.S. Growth and surface morphology of textured NiO thin films deposited by off-axis RF magnetron sputtering. *Jpn. J. Appl. Phys.* 2004. **43**. P. 5524. https://doi.org/10.1143/JJAP.43.5524.

Authors' contributions

Ievtushenko A.I.: key ideas, conceptualization, investigation, writing – original draft, supervision.
Karpyna V.A.: performed experiments of transmittance, analyzing the data.
Bykov O.I.: performed XRD measurements.
Dranchuk M.V.: performed resistivity measurements.
Kolomys O.F.: analyzing the data of RTIR, writing and editing FTIR part.
Maziar D.M.: performed experiments of FTIR.
Strelchuk V.V.: validation of FTIR experimental data.
Starik S.P.: performed SEM and EDX measurements.
Baturin V.A.: sample preparation, thin films ion implantation.
Karpenko O.Yu.: sample preparation, manufacture of ZnO films.
Lytvyn O.S.: performed AFM measurements, analyzing the data, editing.

Authors and CV

Arsenii I. Ievtushenko, PhD in Physics and Mathematics, Head of Department of Physics and Technology of Photoelectronic and Magnetoactive Materials at the I. Frantsevych Institute for Problems of Materials Science, NAS of Ukraine. Author of more than 230 publications. His research interests include solid-state physics, functional materials, physical and chemical properties of oxide semiconductors.
https://orcid.org/0000-0002-8965-6772

Vitalii A. Karpyna, PhD in Physics and Mathematics, Senior Researcher at the Department of Physics and Technology of Photoelectronic and Magnetoactive Materials, I. Frantsevych Institute for Problems of Materials Science, NAS of Ukraine. Author of 154 publications. The main research activity covers the growth of thin films and nanostructures, investigation of these structure, optical and electrical properties of oxide semiconductors. E-mail: v_karpina@ukr.net,
https://orcid.org/0000-0002-1834-3672

Olexander I. Bykov, PhD in Engineering. Leading Researcher at the I. Frantsevych Institute for Problems of Materials Science, NAS of Ukraine. Author of more than 200 publications. His research interests include solid state physics, XRD. https://orcid.org/0000-0001-6959-3498

Mykola V. Dranchuk, Junior Researcher at the I. Frantsevych Institute for Problems of Materials Science, NAS of Ukraine. Author of more than 25 publications. His research interests include solid state physics, Hall measurements.
https://orcid.org/0000-0001-8218-5106

Denys M. Maziar, PhD student at the V. Lashkaryov Institute of Semiconductor Physics, NAS of Ukraine. The area of his research interests includes Raman spectroscopy and FTIR. Also interested in semiconductor thermoelectric converters.

E-mail: fmbfiz13.mazyar@kpnu.edu.ua,
https://orcid.org/0000-0002-8906-6107

Oleksandr F. Kolomys, PhD, Senior Researcher at the Laboratory of submicron optical spectroscopy, V. Lashkaryov Institute of Semiconductor Physics, NASU. Authored over 130 publications, 3 patents, 3 chapters in textbooks. The area of his scientific interests includes Raman and luminescent microanalysis of light emitting properties, structure, composition, electronic and phonon excitations in solids, physical and chemical properties of semiconductors, chemicals and nanostructures with submicron spatial resolution. https://orcid.org/0000-0002-1902-4075

Viktor V. Strelchuk, Doctor of Science in Physics and Mathematics, Professor, Leading Researcher at the Laboratory of submicron optical spectroscopy, V. Lashkaryov Institute of Semiconductor Physics. Authored over 300 publications, 10 patents, 6 textbooks. Field of research: physics of semiconductors, Raman and photoluminescence spectroscopy of semiconductors, nanostructures and nanoscale materials. E-mail: viktor.strelchuk@ccu-semicond.net,
https://orcid.org/0000-0002-6894-1742

Sergii P. Starik, PhD in Materials Science. Head of Laboratory "Nanostructural and crystallophysical researches" at the V. Bakul Institute for Superhard Materials, NASU. Authored over 100 publications, 7 patents. His research interests include diagnostic of physics properties of materials.
https://orcid.org/0000-0003-1991-3275

Volodymyr A. Baturin, PhD in Physics and Mathematics, Member of Academic Council, Principal research assistant, Deputy head of the Department, Head of Laboratory at the Institute of Applied Physics, NASU. The area of scientific interests includes the manufacture of nanostructured materials, physics of nuclei, elementary particles and high energies.
https://orcid.org/0000-0001-6171-8575

Oleksandr Yu. Karpenko, Junior Researcher at the Institute of Applied Physics, NASU. Author of more than 40 publications, 2 patents. Research interests include the influence of surface modification on the probability of high-vacuum breakdown, the technology of thin films, and ion implantation. https://orcid.org/0000-0001-9280-082X

Oksana S. Lytvyn, PhD in Physics and Mathematics, Dean of the Faculty of Information Technologies and Mathematics at the Borys Grinchenko Kyiv University. Author of more than 250 publications, 2 patents, 5 chapters of textbooks. The area of her scientific interests includes theoretical modeling and digital technologies in scanning probe microscopy of physical and mechanical surface properties of various materials.
E-mail: o.lytvyn@kubg.edu.ua,
https://orcid.org/0000-0002-5118-1003

Вплив температури підкладки на структуру та оптичні властивості тонких плівок NiO, осаджених методом магнетронного розпилення в режимі пошарового росту

А.І. Євтушенко, В.А. Карпина, О.І. Биков, М.В. Дранчук, О.Ф. Коломис, Д.М. Мазяр, В.В. Стрельчук, С.П. Старик, В.А. Батурин, О.Ю. Карпенко, О.С. Литвин

Анотація. Якісні полікристалічні плівки NiO є дуже привабливими матеріалами для різних застосувань. Розглянуто вплив температури підкладки на структуру, морфологію та оптичні властивості плівок NiO, осаджених на скляні підкладки методом магнетронного розпилення в режимі пошарового росту. На рентгенограмі виявлено відбиття від (111), (200) і (220) площин кубічного NiO. Продемонстровано, що стехіометричне співвідношення O/Ni наближається до 1,0 з підвищенням температури підкладки. Оптичний коефіцієнт пропускання осаджених плівок NiO був у межах 20–35%, а оптична ширина забороненої зони змінювалася від 2,76 до 2,98 еВ. АСМ аналіз морфології поверхні показав, що середній розмір зерен плівок NiO змінювався від 25 до 30 нм, а шорсткість поверхні від 1,1 до 1,5 нм відповідно.

Ключові слова: плівки NiO, магнетронне розпилення, РФА, температура підкладки, коефіцієнт пропускання, атомно-силова мікроскопія.